

AEDC-TR-67-38

ARCHIVE COPY
DO NOT LOAN



**SOME ASPECTS OF THERMAL MODEL TESTING
IN SPACE CHAMBERS**

K. W. Nutt and J. A. van der Blik
ARO, Inc.

April 1967

Distribution of this document is unlimited.

**AEROSPACE ENVIRONMENTAL FACILITY
ARNOLD ENGINEERING DEVELOPMENT CENTER
AIR FORCE SYSTEMS COMMAND
ARNOLD AIR FORCE STATION, TENNESSEE**

AEDC TECHNICAL LIBRARY



5 0720 00031 4635

PROPERTY OF U. S. AIR FORCE
AEDC LIBRARY
AF 40(600)1200

NOTICES

When U. S. Government drawings specifications, or other data are used for any purpose other than a definitely related Government procurement operation, the Government thereby incurs no responsibility nor any obligation whatsoever, and the fact that the Government may have formulated, furnished, or in any way supplied the said drawings, specifications, or other data, is not to be regarded by implication or otherwise, or in any manner licensing the holder or any other person or corporation, or conveying any rights or permission to manufacture, use, or sell any patented invention that may in any way be related thereto.

Qualified users may obtain copies of this report from the Defense Documentation Center.

References to named commercial products in this report are not to be considered in any sense as an endorsement of the product by the United States Air Force or the Government.

SOME ASPECTS OF THERMAL MODEL TESTING
IN SPACE CHAMBERS

K. W. Nutt and J. A. van der Bliet
ARO, Inc.

Distribution of this document is unlimited.

FOREWORD

The work reported herein was performed at the Arnold Engineering Development Center (AEDC), Air Force Systems Command (AFSC), under Program Element 65402234.

The results of investigations presented were obtained by ARO, Inc. (a subsidiary of Sverdrup & Parcel and Associates, Inc.), contract operator of the AEDC, AFSC, Arnold Air Force Station, Tennessee, under Contract AF 40(600)-1200. The investigations were conducted from May, 1964 to November, 1966, under ARO Project No. SA0412, and the manuscript was submitted for publication on February 6, 1967.

This technical report has been reviewed and is approved.

Donald K. Law
Major, USAF
AF Representative, AEF
Directorate of Test

Leonard T. Glaser
Colonel, USAF
Director of Test

ABSTRACT

Various facets of thermal testing of space vehicles in cold vacuum chambers, with and without solar simulation, are discussed. Emphasis is on thermal modeling of spacecraft. Thermal modeling is discussed for the case of simultaneous preservation of temperature, material and surface properties. The following specific items are treated: (1) a criterion for the application of isothermal modeling is developed and illustrated with experimental data, (2) rules for nonisothermal modeling are discussed and illustrated with experimental results, (3) the effect of internal convection is calculated and modeling rules are developed, (4) the effect of internal radiation is discussed and the relative importance illustrated theoretically, and (5) a criterion is developed for the degree of intensity nonuniformity for a solar simulator in terms of desired temperature accuracy.

CONTENTS

	<u>Page</u>
ABSTRACT.	iii
NOMENCLATURE.	vi
I. INTRODUCTION	1
II. SIMPLIFIED THERMAL MODELING	1
III. ISOTHERMAL BODIES	5
IV. NONISOTHERMAL BODIES	8
V. INTERNAL CONVECTION	9
VI. INTERNAL RADIATION	12
VII. SOLAR SIMULATOR UNIFORMITY CRITERION	14
VIII. CONCLUDING REMARKS	18
REFERENCES	20

ILLUSTRATIONS

<u>Figure</u>		
1.	Experimental Verification of Isothermal Criterion	7
2.	Example of Thin Shell, Nonisothermal Scaling	8
3.	Typical Wall and Gas Temperature as a Function of Time	11
4.	Effect of Gas on the Temperature of a Solid during Transient Conditions.	11
5.	Steady-State Temperature Distribution of a Sphere with Internal Radiation.	13
6.	Solar Simulator Nonuniformity	16
7.	Experimental Data Illustrating Solar Simulator Nonuniformity Effects	19

NOMENCLATURE

A	Dimensionless amplitude of solar simulator nonuniformity
A	Surface area, m^2
a_{hi}, a_{ri}	Reference area, m^2
C	Ratio of heat capacities, $\frac{c_g M_g}{c_s M_s}$
c	Specific heat, Joule/kg - °K
d	Material thickness, m
E	Nondimensional temperature error
$f(\mu)$	Radiation function in Eq. (19)
H_{ij}	Heat transfer coefficient, watt/ m^2 - °K
h	Heat transfer coefficient, watt/ m^2 - °K
h_{ij}	Reference heat transfer coefficient, watt/ m^2 - °K
\bar{h}_{ij}	Nondimensional heat transfer coefficient
K	Scaling ratio
L	Reference length, linear dimension of body, m
ℓ	Half wavelength of solar simulator nonuniformity, m
M	Mass, kg
n	Integer
P	$\frac{\epsilon \sigma A_e}{h A_i} (T_E - T_o)^3$
Q	$\frac{T_o}{T_E - T_o}$
q	Heat flux, watt/ m^2
\bar{q}	Nondimensional heat flux, $\frac{q}{\sigma T_o^4}$
R	Radius, m
S	Internal heat generation, watt/ m^3
T	Temperature, °K
t	Time, sec
V	Volume, m^3
v	Reference volume, m^3

X, Y, Z	Cartesian coordinates, m
a	Absorptivity
a_{hi}, a_{ri}	Nondimensional area
Γ	Nonuniformity parameter, Eq. (21)
γ	Conduction parameter, Eq. (19)
δ	Ratio of emissivities, ϵ_i/ϵ_e
ϵ	Surface emissivity
θ	Nondimensional temperature
λ	Thermal conductivity, watt/m - °K
μ	Cos ν
ν	Polar angle for sphere
ξ, η, ζ	Nondimensional coordinates in x-, y-, and z-direction
ρ	Density, kg/m ³
σ	Stefan-Boltzmann constant, watt/m ² - (°K) ⁴
τ	Nondimensional time
ϕ	Nondimensional solar simulator intensity, $\frac{q}{q_s}$
ϕ_i	Nondimensional volume

SUBSCRIPTS

E	Equilibrium
e	External
g	Gas
h	Convection or conduction surface
i	Internal
i, j	Numerals
m	Model
o	Reference, initial, outside
p	Prototype
r	Reference, radiation surface
s	Solar, solid

SECTION I INTRODUCTION

Thermal model testing of space vehicles and associated components has increased because full-scale environmental tests have become more difficult to accommodate in existing ground test facilities. This approach requires that a thermal model must be designed that will accurately predict the thermal response of the full-scale prototype. To accomplish the practical design of thermal models, sufficient experience must be gained to ensure that the modeling techniques used will predict the thermal behavior of the prototype.

Thermal model testing has been the subject of several papers during the last few years. In particular, thermal scale modeling was discussed by Vickers (Ref. 1) and Wainwright (Ref. 2). A thorough treatment of thermal modeling rules was given by Chao and Wedekind (Ref. 3), and Jones (Ref. 4) derived an extensive set of similarity ratios to be preserved when several bodies, each having its own characteristic temperature, are scaled together.

The object of this study is to discuss several aspects of thermal model testing in space simulation chambers. The subjects discussed include: a criterion for the application of isothermal modeling rules, the application of nonisothermal modeling rules, the effect of internal convection and internal radiation on the thermal balance of a model, and a criterion to determine the degree of intensity nonuniformity for a solar simulator in terms of desired temperature accuracy. By treating these aspects of thermal modeling separately, and correlating this with previous work (Refs. 1-4), it is intended that a practical technique of thermal model testing will be implemented.

SECTION II SIMPLIFIED THERMAL MODELING

The heat conduction equation in body number i of an assembly of n bodies is

$$\rho_i c_i \frac{\partial T_i}{\partial t} = \text{div} (\lambda_i \text{grad } T_i) + S_i \quad (1)$$

where S_i is the internal heat generation per unit volume. Radiation heat exchange at the boundary is expressed by the condition

$$\lambda_i \left(\frac{\partial T_i}{\partial Z_i} \right)_{\text{boundary}} = q_{i, \text{net}} \quad (2)$$

where Z_i is the coordinate normal to the surface and $q_{i, net}$ is the net radiative heat flux per unit area. The general form of this heat flux has been discussed by Chao (Ref. 3). The quantity $q_{i, net}$ may include contributions from solar radiation, albedo, and earth radiation as well as radiation from other bodies and other parts from the same body, externally or internally.

In this report the external prototype and model* geometry are assumed to be similar. Also the radiative surface properties are preserved in scaling. Furthermore, if the temperature at homologous points is the same on model and prototype, effects of changes in surface emissivity or absorptivity with temperature do not enter into the scaling problem. In general, this state can be achieved only if the model has the same surface finish as the prototype.

If the internal heat generation term, S_i , is neglected, the non-dimensional form of Eqs. (1) and (2) is

$$\left. \begin{aligned} \frac{\partial \theta_i}{\partial \tau} &= \frac{\lambda_i t_o}{\rho_i c_i L^2} \left[\left(\frac{\partial^2}{\partial \xi^2} + \frac{\partial^2}{\partial \eta^2} + \frac{L^2}{d^2} \frac{\partial^2}{\partial \zeta^2} \right) \theta_i \right] \\ \left(\frac{\partial \theta_i}{\partial \zeta} \right)_{\text{boundary}} &= \frac{\sigma T_o^3 d}{\lambda_i} \bar{q}_i \end{aligned} \right\} \quad (3)$$

where

$$\begin{aligned} T &= \theta T_o & X &= \xi L \\ t &= \tau t_o & Y &= \eta L \\ q_i &= \bar{q} \sigma T_o^4 & Z &= \zeta d \end{aligned}$$

The coordinates X and Y are along the surface and are scaled in the same ratio, whereas the coordinate Z can be scaled in a different ratio, allowing a minor geometric distortion.

Vickers (Ref. 1) stated that it is not possible to carry out thermal modeling with preservation of material, surface finish, and temperature if the model has complete geometric similarity. This is shown by listing the similarity parameters, from Eq. (3), to be preserved between prototype and model:

$$\left(\frac{\lambda_i t_o}{\rho_i c_i L^2} \right), \quad \left(\frac{L}{d} \right), \quad \left(\frac{\sigma T_o^3 d}{\lambda_i} \right)$$

*The term prototype is used to designate the space vehicle, and the term model refers to a scaled (larger or smaller) version of the space vehicle.

Since it is extremely attractive to preserve both temperature, as explained above, and materials in thermal scaling, minor geometric distortions are introduced where possible. If the temperature field is essentially two-dimensional, the boundary condition in Eq. (3) can be introduced in the differential equation

$$\frac{\partial \theta_i}{\partial \tau} = \frac{\lambda_i t_o}{\rho_i c_i L^2} \left[\left(\frac{\partial^2}{\partial \xi^2} + \frac{\partial^2}{\partial \eta^2} \right) \theta_i + \frac{L^2}{d} \frac{\sigma T_o^3}{\lambda_i} \bar{q}_i \right] \quad (4)$$

and the similarity parameters are

$$\left(\frac{\lambda_i t_o}{\rho_i c_i L^2} \right), \left(\frac{L^2}{d} \frac{\sigma T_o^3}{\lambda_i} \right)$$

or for material and temperature preservation, the ratios

$$\left(\frac{t_o}{L^2} \right) \text{ and } \left(\frac{L^2}{d} \right) \quad (5)$$

have to be preserved. This thin shell approximation was given in Refs. 2 and 3 and experimentally verified in Ref. 5.

If the bodies or parts of the bodies to be scaled can be considered isothermal, another set of similarity rules can be derived, affording more freedom than given by Eq. (5). Isothermal bodies have been considered in detail by Jones (Ref. 4). Here a simple derivation is given, starting from Eq. (1) and assuming at the onset that external radiation scaling is satisfied by using similar geometries and identical surface properties and neglecting S_i . The right-hand side of Eq. (1) now consists of two parts - (1) heat transfer through a surface A_h from another body j adjacent to the body i with a heat transfer coefficient H_{ij} and (2) radiation transfer through a surface A_r with the flux $q_i = q_{i, \text{net}}$ replacing the boundary condition Eq. (2). Therefore, for n bodies,

$$\rho_i c_i V_i \frac{dT_i}{dt} = \sum_{\substack{j=1 \\ j \neq i}}^{j=n} H_{ij} A_{hi} (T_j - T_i) - q_i A_{ri} \quad (6)$$

Using the nondimensional notation as before and in addition

$$\begin{aligned} V_i &= \phi_i v_i & A_{hi} &= \alpha_{hi} a_{hi} \\ H_{ij} &= \bar{h}_{ij} h_{ij} & A_{ri} &= \alpha_{ri} a_{ri} \end{aligned}$$

Equation (6) becomes

$$\phi_i \frac{d\theta_i}{d\tau} = \left(\frac{h_{ij} a_{hi} t_o}{\rho_i c_i v_i} \right) \sum_{\substack{j=1 \\ j \neq i}}^{j=n} \bar{h}_{ij} \alpha_{hi} (\theta_j - \theta_i) + \left(\frac{\sigma T_o^3 a_{ri} t_o}{\rho_i c_i v_i} \right) \bar{q}_i \alpha_{ri} \quad (7)$$

and the similarity parameters to be preserved are

$$\left(\frac{h_{ij} a_{hi} t_o}{\rho_i c_i v_i} \right) \quad \text{and} \quad \left(\frac{\sigma T_o^3 a_{ri} t_o}{\rho_i c_i v_i} \right)$$

Material and temperature preservation reduce this further to

$$\left(\frac{h_{ij} a_{hi} t_o}{v_i} \right) \quad \text{and} \quad \left(\frac{a_{ri} t_o}{v_i} \right)$$

If the prototype is scaled by a factor K, the external surface area, a_{ri} , will be scaled by a factor K^2 for geometric similarity required by radiation exchange. The last parameter in Eq. (8) gives, then,

$$\frac{(t_o)_m}{(t_o)_p} = \frac{(a_{ri})_p}{(a_{ri})_m} \frac{(v_i)_m}{(v_i)_p} = \frac{1}{K^2} \frac{(v_i)_m}{(v_i)_p}$$

This introduces some freedom in selecting the time scale:

- (a) If $(t_o)_m = (t_o)_p$ is selected, the volume must be scaled by K^2 , which is possible by leaving the material thickness unchanged. This was done in Ref. 6 where the volume (and heat capacity) was scaled by a factor K^2 . The first parameter in Eq. (8) gives, now,

$$(h_{ij} a_{hi})_m = K^2 (h_{ij} a_{hi})_p$$

In general, one dimension of the cross section, a_{hi} , will be along the external surface and one dimension will be in the direction of the thickness, so that $(a_{hi})_m = K(a_{hi})_p$ and therefore

$$(h_{ij})_m = K(h_{ij})_p$$

The model has to be divided into isothermal parts separated by junctions with heat transfer coefficients smaller than the original ones in the case of $K < 1$; i. e., additional thermal resistance has to be introduced. When there is only radiative heat transfer between the isothermal parts, only the last parameter in Eq. (8) has to be satisfied.

- (b) If $(t_o)_m = K(t_o)_p$ is selected, the volume scaling is $(V_i)_m = K^3(V_i)_p$, and the model is scaled equally in all directions. The heat transfer coefficients are now scaled according to

$$\frac{(h_{ij})_m}{(h_{ij})_p} = \frac{(v_i)_m}{(v_i)_p} \frac{(t_o)_p}{(t_o)_m} \frac{(a_{hi})_p}{(a_{hi})_m} = K^3 \cdot \frac{1}{K} \cdot \frac{1}{K^2} = 1$$

The heat transfer coefficients remain unchanged.

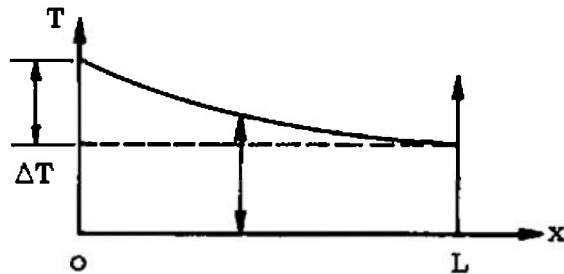
(c) If $(t_o)_m = K^2(t_o)_p$, the volume is scaled by K^3 and the heat transfer coefficients are scaled by

$$\frac{(h_{ij})_m}{(h_{ij})_p} = \frac{(v_i)_m}{(v_i)_p} \frac{(t_o)_p}{(t_o)_m} \frac{(a_{hi})_p}{(a_{hi})_m} = K^4 \cdot \frac{1}{K^2} \cdot \frac{1}{K^3} = \frac{1}{K}$$

This is the same result as that obtained with the thin shell approximation where the thermal resistance is scaled by a factor K automatically.

SECTION III ISOTHERMAL BODIES

In order to apply isothermal modeling rules, it has to be decided when a body or part of a body can be considered isothermal. If at any time the ratio $\frac{\Delta T}{T} \ll 1$, the body is said to be isothermal. Here ΔT is a typical temperature difference, say, between the hottest and coldest point on the body. An equivalent statement is



$$\frac{\partial T_i}{\partial x_i} L_i \ll 1 \tag{9}$$

where L_i is a typical length in the direction of x_i . It follows from the heat conduction Eq. (1) that

$$\text{grad } T = 0 \left(\frac{\rho c}{\lambda} L \frac{\partial T}{\partial t} \right)^* \tag{10}$$

It is assumed that the internal heat generation can be neglected. Combining Eqs. (9) and (10) leads to the condition to be satisfied for the isothermal assumption:

$$\frac{\rho c}{\lambda} \frac{L^2}{T} \frac{\partial T}{\partial t} \ll 1$$

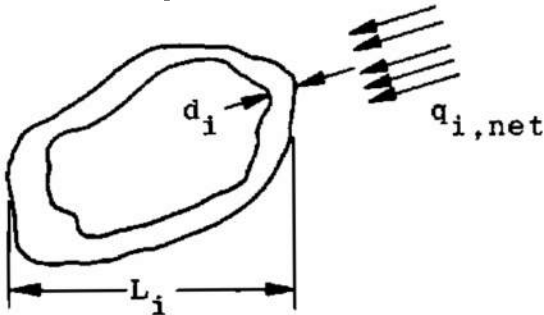
or, also,

$$\frac{\rho c}{\lambda} \frac{L^2}{t_o} \ll 1 \tag{11}$$

where t_o is a typical time, for instance the period in a test with cyclic solar simulation.

*The notation $0(\dots\dots)$ means: on the order of $(\dots\dots)$

Condition (11) applies to the overall length of a body shown in the accompanying sketch. This condition is certainly satisfied for a minor



dimension, such as the thickness \$d\$. However, if solar radiation in one side of the body provides the heat input, the boundary condition of Eq. (2) gives an additional requirement. From Eq. (9),

$$\frac{\text{grad}(T) \cdot d}{T} \ll 1$$

and with (Eq. 2),

$$\frac{(q_{i,net}) d_i}{\lambda T} \ll 1 \tag{12}$$

As an example, the requirements for isothermal bodies are listed below, with \$T = 300^\circ\text{K}\$, \$q_{i,net} = 0.14 \text{ watt/cm}^2\$ (solar radiation), and \$t_o = 100 \text{ min}\$ (orbital period):

Material	Copper	Aluminum	Stainless Steel
\$\lambda\$, watt/cm-\$^\circ\text{K}\$	4.0	1.0	0.13
\$\lambda/\rho c\$, cm\$^2\$/sec	1.1	0.44	0.04
\$d\$, cm \$\ll\$	8600	2150	280
\$L^2\$, cm\$^2\$ \$\ll\$	6600	2640	240

It is concluded from this table that, even for materials with a high thermal conductivity, truly isothermal conditions are only achieved for very small bodies, say, with a length \$L = 10\$ to \$30 \text{ cm}\$ for copper.

The isothermal criterion is illustrated by experiments reported in Ref. 6. Three bodies - a plate, a cylinder, and a sphere - were placed in a cold vacuum chamber (Fig. 1). In this case the plate was heated periodically. The extreme temperatures of the aluminum cylinder, heated by radiation from the plate, were equal within a few degrees (Fig. 1a). On the other hand, the extreme temperatures of the stainless steel sphere differed as much as \$140^\circ\text{K}\$ (Fig. 1b). The parameter \$\frac{\rho c}{\lambda} \frac{L^2}{t_o}\$ was equal to 0.06 in the former and 1.6 in the latter case. Since in the latter case the isothermal condition was not met, a scaling procedure based on the assumption that each of the three bodies was isothermal did not result in an accurate prediction of prototype temperatures from

a thermal model experiment. This point was demonstrated in Ref. 6. Even an aluminum sphere would not quite meet the isothermal requirement [Eq. (11)].*

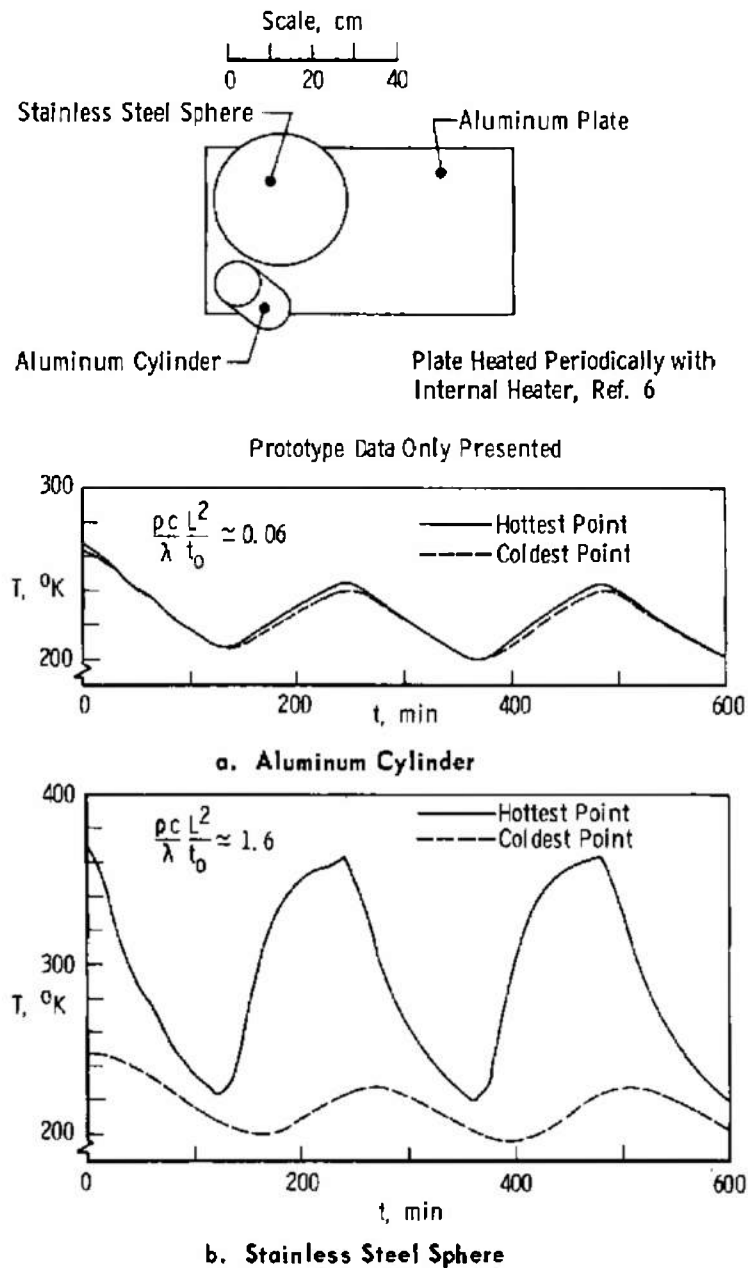


Fig. 1 Experimental Verification of Isothermal Criterion

*In Ref. 6, test results with an aluminum sphere are given, but in that test the sphere also had an internal heater to help produce uniform temperatures.

**SECTION IV
NONISOTHERMAL BODIES**

When the same configuration, with a stainless steel sphere, was scaled using the thin shell approximation, i. e., scaling was carried out on the basis of thermal resistance rather than thermal capacity, good agreement between homologous temperatures on the model and prototype was obtained (Ref. 5).

Another example of the use of the thin shell (two dimensional) modeling rules given by Eq. (5) is shown in Fig. 2, where typical temperatures of a prototype and a half-scale model are compared. In this case, the bodies were heated periodically with a carbon arc solar simulator in a cold (77°K) vacuum chamber.

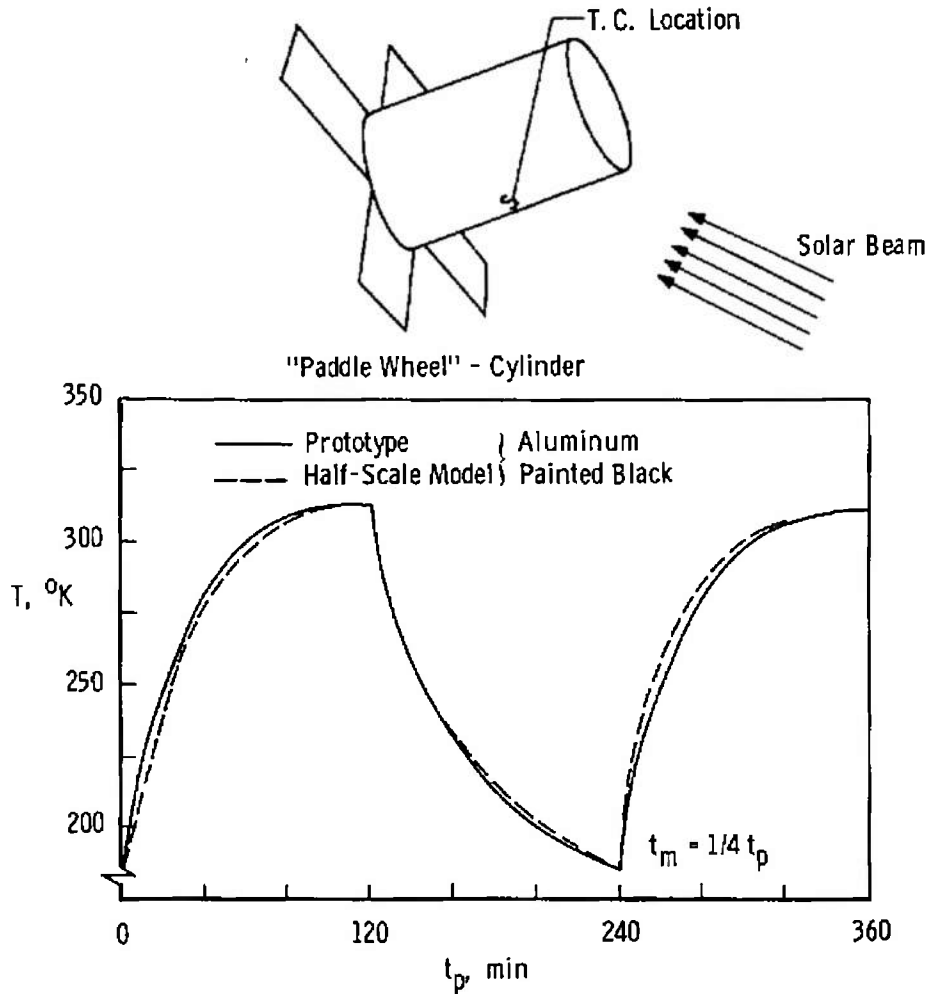


Fig. 2 Example of Thin Shell, Nonisothermal Scaling

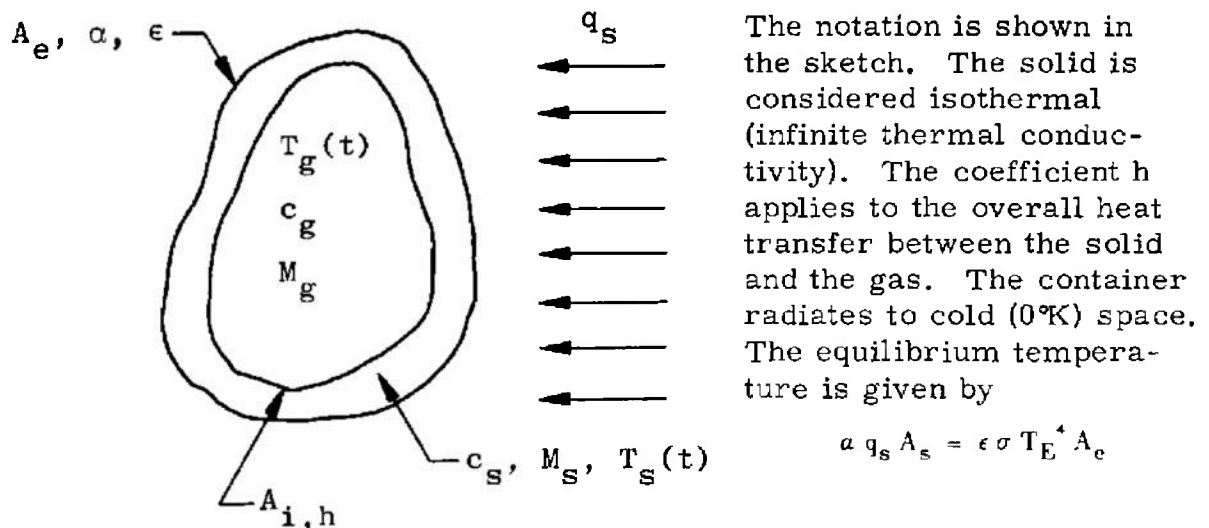
SECTION V INTERNAL CONVECTION

In thermal testing of space vehicles, the gas (or liquid) in the vehicle may significantly influence the heat balance and the temperature-time history. Tests carried out in a space chamber with gravity-induced convection do not simulate free-space conditions. Only a facility for testing free-fall models would properly simulate zero gravity conditions. While it is clear that the liquid in a thin-walled tank influences, markedly, the temperature-time history of such a tank when it is subjected to a periodic solar source in cold space, it is not immediately apparent when the heat capacity of a gas and the heat transmission through the gas are important. The following derivation is therefore given primarily to establish the limits for negligible convection effects.

The heat balance equations for the gas and a solid container of arbitrary shape, as sketched below, are

$$\alpha q_s A_s - \epsilon \sigma T_s^4 A_e - h (T_s - T_g) A_i = c_s M_s \frac{dT_s}{dt} \quad (13)$$

$$h (T_s - T_g) A_i = c_g M_g \frac{dT_g}{dt} \quad (14)$$



where A_s is the projected surface area normal to the solar beam direction and T_E is the final equilibrium temperature.

Equations (13) and (14) can be written in nondimensional form:

$$P [(1 + Q)^4 - (\theta_s + Q)^4] - (\theta_s - \theta_g) = \frac{d\theta_s}{d\tau} \quad (15)$$

$$\theta_s - \theta_g = C \frac{d\theta_g}{d\tau} \quad (16)$$

where

$$\left. \begin{aligned} \theta_s &= \frac{T_s - T_o}{T_E - T_o} & \theta_g &= \frac{T_g - T_o}{T_E - T_o} & r &= \frac{t}{\left(\frac{c_g M_g}{h A_i}\right)} \\ \text{and} & & & & & \\ C &= \frac{c_g M_g}{c_s M_s} & P &= \frac{\epsilon \sigma A_e}{h A_i} (T_E - T_o)^3 & Q &= \frac{T_o}{T_E - T_o} \end{aligned} \right\} \quad (17)$$

This set of equations was solved numerically for the following boundary conditions:

$$\begin{aligned} \text{At } \tau = 0 & : \theta_g = \theta_s = 0 \\ \text{At } \tau \rightarrow \infty & : \theta_g = \theta_s = 1 \end{aligned}$$

A typical solution is shown in Fig. 3. The results of calculations for various values of C, P, and Q are summarized in Fig. 4, which is a plot of the decrease in θ_s at $\theta_s = 0.8$ that was attributable to the presence of the gas versus C (the ratio of thermal capacity of the gas to that of the container) with P and Q as parameters.

For a sphere of 1-m diameter filled with air at 1 to 100 atm at room temperature, it was estimated that $h = 3$ to 30 watt/m² °K. With $\epsilon = 1.0$ and $A_e/A_i = 1$, this gives $P = 0.05$ to 0.5 . A metal sphere of 1-m diameter and thickness of one hundredth of its diameter, filled with air at 1 atm has a value of C on the order of 0.01.

For the cases considered, $\Delta\theta_s < 0.5C$, and thus for "ordinary" conditions it is expected that the effect of the gas on the temperature of the solid is very small (a few degrees) and probably within the measuring accuracy for many tests. Under space conditions, the heat transfer coefficient, h , is expected to be considerably smaller than in a space chamber; therefore, P will be larger, which tends to reduce the effect of the gas further.

Figure 4 helps to set the limits when convection can be neglected. However, it is interesting to consider convection scaling parameters. From Eqs. (15) and (16) it follows that C, P, and Q, together with the

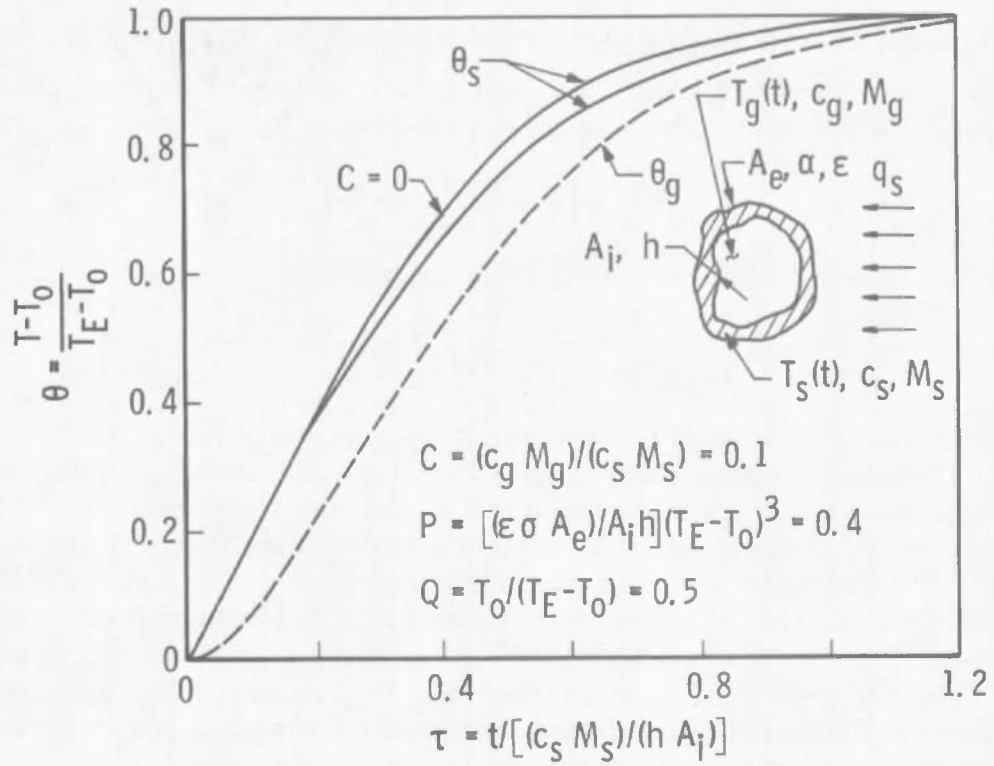


Fig. 3 Typical Wall and Gas Temperature as a Function of Time

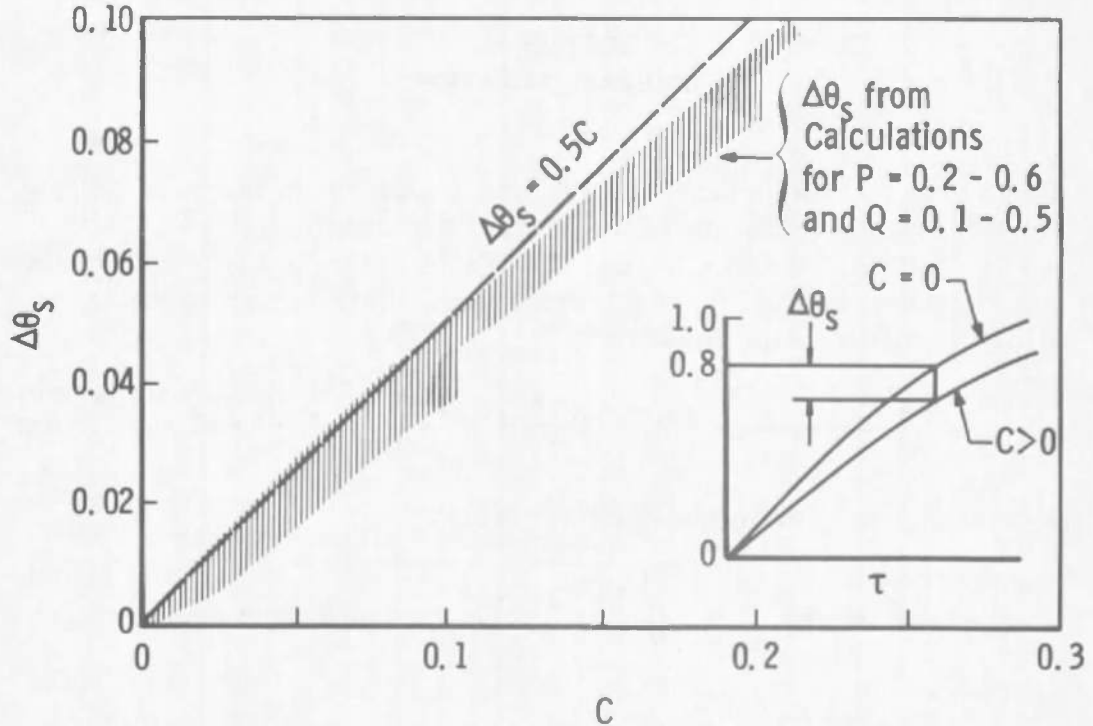


Fig. 4 Effect of Gas on the Temperature of a Solid during Transient Conditions

characteristic time $t_r = \frac{c_s M_s}{h A_i}$ are the similarity parameters. Making the same restrictions as before - temperature and surface properties preservation - the similarity parameters become

$$\left(\frac{c_g M_g}{c_s M_s} \right), \left(\frac{A_e}{h A_i} \right), \left(\frac{c_s M_s}{t_r h A_i} \right)$$

Since for similarity $h A_i \sim A_e$, one can also write

$$\left(\frac{c_g M_g}{c_s M_s} \right), \left(\frac{A_e}{h A_i} \right), \left(\frac{c_s M_s}{A_e t_r} \right) \tag{18}$$

The first parameter appears to cause no special problems. Since it is expected that under space conditions h is much smaller than under laboratory conditions, the internal area of the model has to be reduced or h has to be reduced by placing internal low conductivity partitions in the model. If in the third parameter c_s remains unchanged, then for a thin shell $M_s \sim K^2$ (surface) $\times K^2$ (thin shell) and $A_e \sim K^2$ so that the time scale is proportional to K^2 . On the other hand, if the body were scaled isothermally, $M_s \sim K^2$ and the time would not be scaled. Thus, convection scaling does not lead to requirements conflicting with other thermal scaling parameters, at least under the present simplifying assumptions.

SECTION VI INTERNAL RADIATION

To assess the importance of internal radiation in thermal testing, the temperature distribution of a sphere with an internally radiating surface is studied. When a hollow sphere is subjected to solar radiation, as sketched in Fig. 5, the temperature distribution is given by the following differential equation:

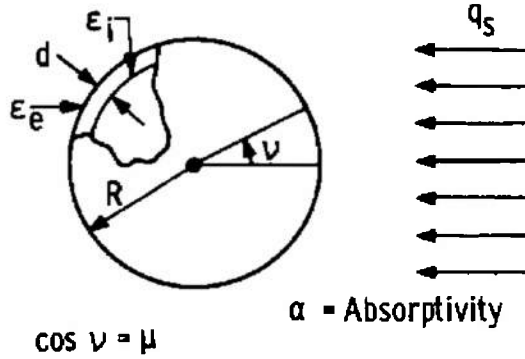
$$\frac{\partial^2 T}{\partial \nu^2} + \cot \nu \frac{\partial T}{\partial \nu} + \frac{\alpha R^2}{\lambda d} f(\nu) q_s \cos \nu - (\epsilon_i + \epsilon_e) \frac{\sigma R^2}{\lambda d} T^4 + \frac{\epsilon_i \sigma R^2}{2\lambda d} \int_0^\pi T^4 \sin \xi d\xi - \rho c \frac{R^2}{\lambda} \frac{\partial T}{\partial t} = 0$$

By introducing the nondimensional variables,

$$\theta = \frac{T}{T(1)} \quad \text{where } T(1) = \sqrt[4]{\frac{1 + \delta/4}{1 + \delta} \left(\frac{\alpha}{\epsilon_e} \right) \left(\frac{q_s}{\sigma} \right)} = \text{temperature at } \nu = 0$$

$$\tau = \frac{t}{t_0}, \quad \text{with } t_0 = \frac{\rho c R^2}{\lambda}$$

Hollow Sphere



$$\delta = \frac{\epsilon_i}{\epsilon_e} \quad \gamma = \frac{\lambda d T(1)}{1 + \left(\frac{\delta}{4}\right) \alpha q_s R^2} \quad \theta = \frac{T}{T(1)} \quad T(1) = \left[\frac{4 + \delta}{4 + 4\delta} \left(\frac{\alpha}{\epsilon_e}\right) \left(\frac{q_s}{\sigma}\right) \right]^{1/4}$$

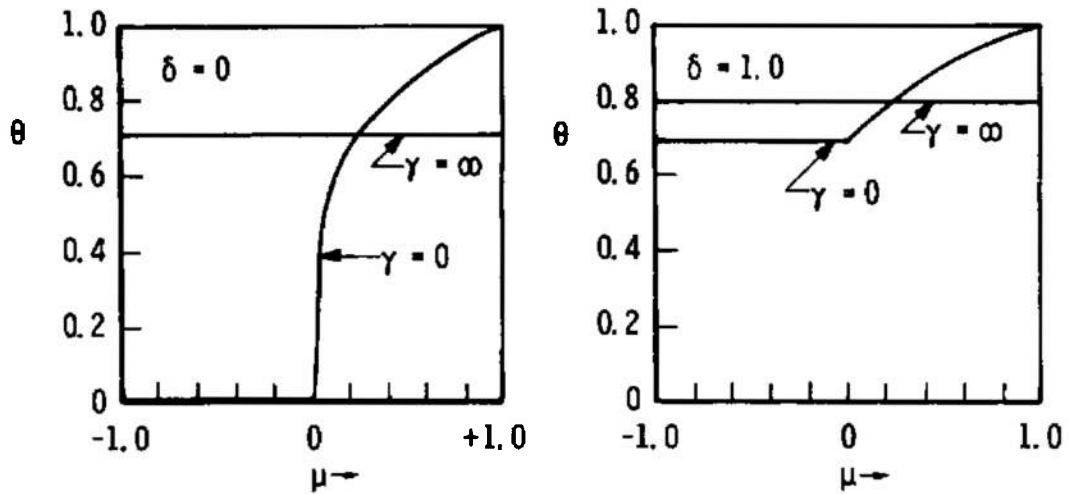


Fig. 5 Steady-State Temperature Distribution of a Sphere with Internal Radiation

and using the notation

$$\mu = \cos \nu$$

$$\gamma = \frac{\lambda d T(1)}{(1 + \delta/4) a q_s R^2} \quad \delta = \frac{\epsilon_i}{\epsilon_e}$$

this reduces to

$$\gamma \left[(1 - \mu^2) \frac{\partial^2 \theta}{\partial \mu^2} - 2\mu \frac{\partial \theta}{\partial \mu} \right] + \frac{\mu f(\mu) + \delta/4}{1 + \delta/4} - \theta = \gamma \frac{\partial \theta}{\partial \tau} \quad (19)$$

The function $f(\mu)$ is $f(\mu) = 1$ for $0 < \mu \leq 1$ and $f(\mu) = 0$ for $-1 \leq \mu < 0$, and accounts for the directional effect of the solar source. The derivation of Eq. (19) is rather long and is presented here only to bring out the influence of internal radiation.

For thermal scaling, the parameters γ and δ have to be preserved. If surface properties are preserved, the reference temperature $T(1)$ is preserved; and if material properties are preserved, the parameters γ and δ reduce to the requirement that $\frac{d}{R^2}$ be preserved. Thus, if $\frac{R_m}{R_p} = K$, the thickness is scaled by $\frac{dm}{dp} = K^2$ and the time is scaled by $\frac{(t_o)_m}{(t_o)_p} = \left(\frac{R_m}{R_p} \right)^2 = K^2$.

This is the same scaling result as that obtained with the thin shell approximation, since the same assumptions are involved. Without going into detailed numerical solutions, it suffices here to plot the temperature distribution along the surface of the sphere for the two cases: $\delta = \frac{\epsilon_i}{\epsilon_e} = 0$ and 1 (Fig. 5). The case of $\gamma = 0$ corresponds to zero conductivity in the sphere wall, and $\gamma = \infty$ is the case of infinite conductivity or an isothermal sphere. It is concluded that the internal radiation properties of a spacecraft model would have to be reproduced accurately in model testing, in particular where complicated internal arrangements occur since corrections would then be difficult to make.

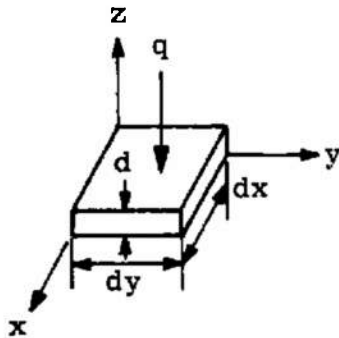
SECTION VII SOLAR SIMULATOR UNIFORMITY CRITERION

The degree of simulation achieved by a solar simulator is a function of how accurately certain characteristics of the actual solar source are simulated. One of these characteristics is the uniformity of the solar simulator beam intensity.

In a general way, the degree of nonuniformity that can be tolerated in a simulated solar beam depends on the test model geometry, the model material, and the allowable error in the temperature distribution. A simplified case will be considered as an initial step in the development of a general solar simulator intensity uniformity criterion.

Since nonuniformity effects are expected to be most severe for thin shells and since most spacecraft are constructed of plate material, consider the heat balance for a flat plate exposed to radiation in the z-direction. Assume no heat flow in the y- and z- directions. The former implies a two-dimensional geometry of both the model and the solar intensity nonuniformities, whereas the latter is the thin shell approximation. With these assumptions,

$$\rho c \frac{\partial T}{\partial t} = \lambda \frac{\partial^2 T}{\partial X^2} + \frac{1}{d} (q - \epsilon \sigma T^4)$$



where d is the material thickness. Using the nondimensional variables introduced in Eq. (3) for T , t , and X , while introducing the additional nondimensional variable $\phi = q/q_s$, gives

$$\frac{\partial \theta}{\partial \tau} = \left(\frac{\lambda t_o}{\rho c l^2} \right) \frac{\partial^2 \theta}{\partial \xi^2} + \left(\frac{q_s t_o}{\rho c T_o d} \right) \phi - \left(\frac{\epsilon \sigma T_o^3 t_o}{\rho c d} \right) \theta^4 \quad (20)$$

As a first approximation to a general nonuniformity criterion for solar simulation, Eq. (20) will be solved in a simplified form. For this, assume that

- (1) $\frac{\partial \theta}{\partial \tau} = 0$, steady-state condition,
- (2) the last term in Eq. (2) is negligible, and
- (3) $\phi = \phi(\xi)$. In general, $\phi = \phi(\xi, \tau)$.

With the above assumptions, Eq. (20) becomes

$$\frac{\partial^2 \theta}{\partial \xi^2} + \Gamma \phi = 0 \quad ; \quad \Gamma = \frac{q_s l^2}{\lambda d T_o} \quad (21)$$

Since ϕ is equal to the ratio of the simulated radiation intensity to the average solar radiation constant, the term Γ can be called the intensity nonuniformity parameter. The magnitude of this term dictates the nonuniformities in the solar simulator intensity that can be tolerated for given allowable temperature tolerances.

As an illustration, assume that $\phi = (1 + A \sin \xi \pi)$. The degree of nonuniformity, $A = \frac{q_{max}}{q_0} - 1$, is as shown in Fig. 6. Equation (21) becomes

$$\frac{\partial^2 \theta}{\partial \xi^2} + \Gamma (1 + A \sin \xi \pi) = 0$$

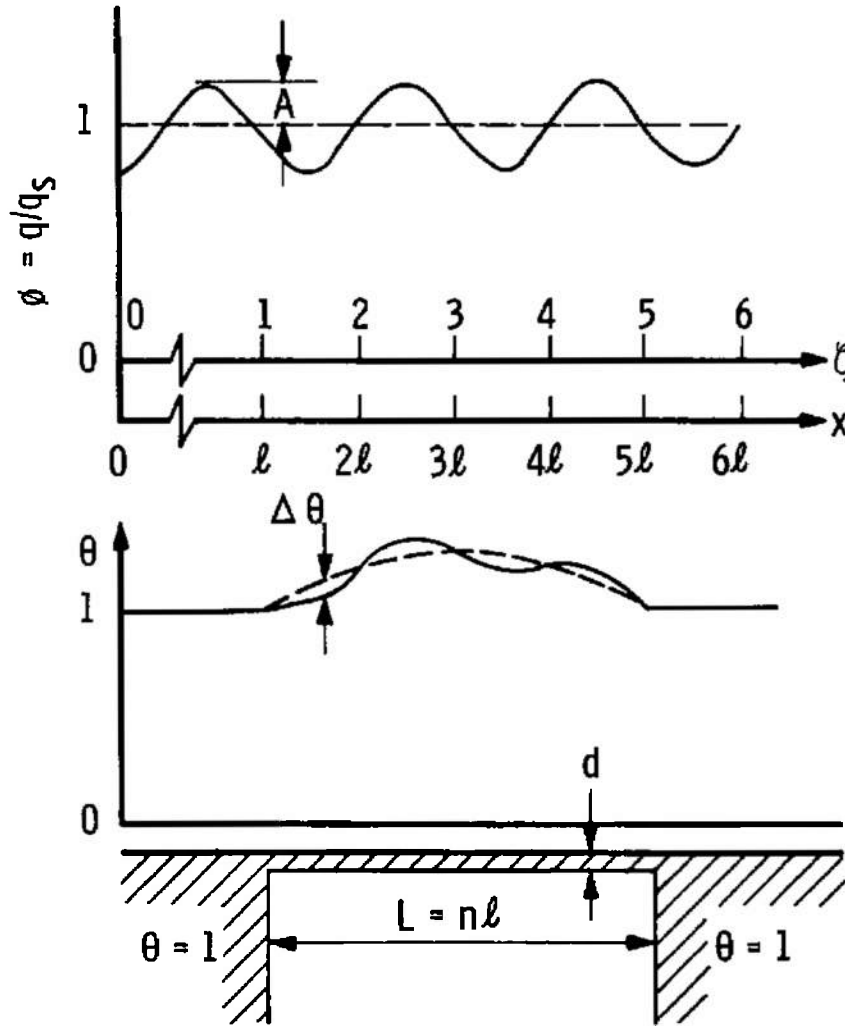


Fig. 6 Solar Simulator Nonuniformity

Considering the case of a plate with a constant temperature at both ends (Fig. 6), the solution is

$$\theta = \frac{A\Gamma}{\pi^2} \sin \xi \pi - \frac{1}{2} \Gamma \xi^2 + \frac{\eta}{2} \Gamma \xi + 1$$

The dashed line on the graph in Fig. 6 is the ideal temperature distribution with a uniform beam intensity ($A=0$) and the solid line is the distribution with a nonuniform intensity ($A \neq 0, n \neq 0$). The error in temperature

at any particular point is

$$E = (\theta)_{A \neq 0} - (\theta)_{A=0} = \frac{A\Gamma}{\pi^2} \sin \xi \pi$$

and

$$E_{\max.} = \frac{\Gamma A}{\pi^2} \quad (22)$$

Since $n\ell = L$, it follows from Eqs. (21) and (22) that

$$E_{\max.} = \frac{\Delta T}{T_c} = \frac{1}{\pi^2} \frac{q_s L^2}{\eta^2 \lambda d T_c} A \quad (23)$$

As n approaches infinity, $E_{\max.}$ approaches zero regardless of A . This shows that if the model dimensions are large compared to the size of the intensity nonuniformities, the error in temperature becomes small. Assuming

$$L = 100 \text{ cm}, n = 10, \ell = 10 \text{ cm}, d = 0.3 \text{ cm}, \text{ and } q_s = 0.14 \text{ watt/cm}^2$$

gives

$$A = \frac{q_{\max.}}{q_s} - 1 = \left(\frac{\eta^2 \pi^2 d}{q_s L^2} \right) \lambda \Delta T = 0.221 \lambda \Delta T$$

So that per degree Kelvin error ($\Delta T = 1^\circ\text{K}$), the maximum allowable intensity nonuniformity is as shown below:

	Copper	Aluminum	Stainless Steel
λ , watt/cm-°K	4.0	1.0	0.13
$A/\Delta T$, percent	±88.4	±22.1	±2.9

The importance of geometry of the model, the solar intensity uniformity, and the material properties are demonstrated by Eq. (23) and the table above.

Thermal modeling tests have been conducted with a carbon arc solar simulator with two different model configurations. The same solar simulator was used in both cases. The models in one test were fabricated from stainless steel, whereas the models used in the second test were fabricated from aluminum sheet. The test articles fabricated with aluminum had a thickness that was double the thickness of the stainless steel models, resulting in a higher value of thermal conductance. Referring to the intensity nonuniformity parameter as incorporated in Eq. (23) and considering that the same solar simulator was

used on both series of tests, gives

$$\frac{(\Delta T)_{S.S.}}{(\Delta T)_{Al}} = \frac{(\lambda d)_{S.S.}}{(\lambda d)_{Al}} = \frac{(1.0)(0.125)}{(0.13)(0.065)} = 14.8$$

This shows that the error that could be expected between analogous temperatures on the scale model and prototype would be approximately 15 times greater with the test articles made of stainless steel than for those fabricated from aluminum. Typical temperatures are plotted in Fig. 7 for the stainless steel and aluminum test articles, where this ratio is only five. It is noted that the last term in Eq. (20) tends to reduce the effects of intensity nonuniformities on temperature distribution. The effect of this term and two-dimensional heat conduction during time-periodic heating contribute to the above discrepancy.

SECTION VIII CONCLUDING REMARKS

The emphasis in this report has been on thermal modeling with simultaneous preservation of temperature, surface properties, and materials. It is felt that for a complicated model this is the most practical method. When the bodies cannot be divided into isothermal parts in a convenient manner, the nonisothermal scaling may introduce impractical material thicknesses, particularly when the model is to be significantly smaller than the prototype. In such a case, much can be learned from partial scaling, for instance on two or three different models, and extrapolation to the correct scaled size. Tests with two or three different materials may also provide useful data for this extrapolation.

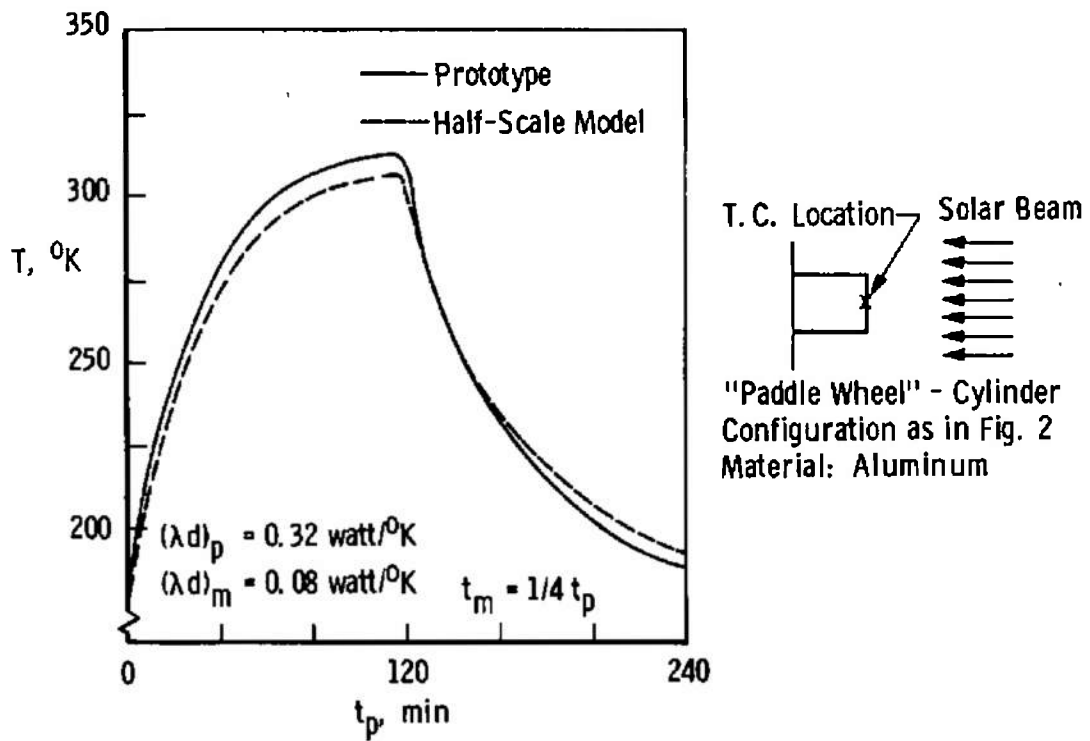
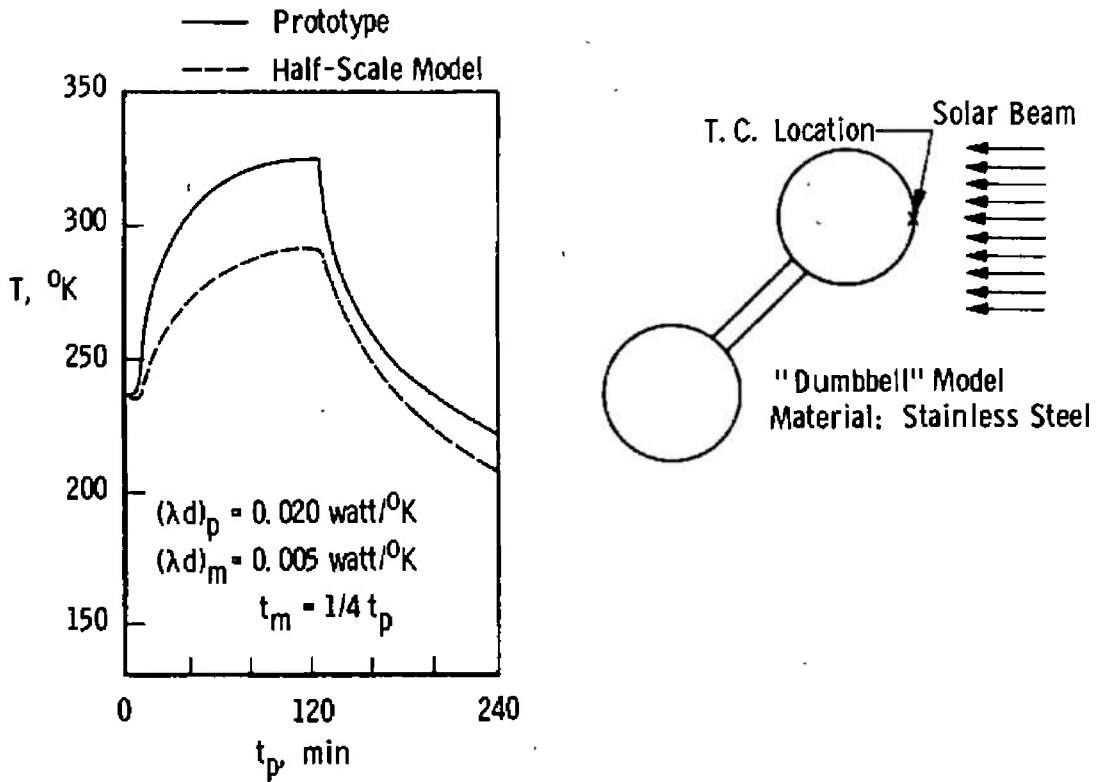


Fig. 7 Experimental Data Illustrating Solar Simulator Nonuniformity Effects

REFERENCES

1. Vickers, J. M. F. "Thermal Scale Modeling." Astronautics and Aeronautics, May, 1965, pp. 34-39.
2. Wainwright, J. B., et al. "Modeling Criteria and Testing Techniques for the Simulation of Space Environments." AFFDL-TR-64-164, October, 1964 (University of Southern California).
3. Chao, B. T. and Wedekind, G. L. "Similarity Criteria for Thermal Modeling of Spacecraft." J. of Spacecraft and Rockets, March-April, 1964, pp. 146-152.
4. Jones, B. P. "Thermal Similitude Studies." J. of Spacecraft and Rockets, July-August, 1964, pp. 364-369.
5. Adkins, D. L. "Scaling of Transient Temperature Distributions of Simple Bodies in a Space Chamber." Thermophysics and Temperature Control of Spacecraft and Entry Vehicles, Ed. by G. B. Heller, Academic Press, New York, 1966.
6. Jones, B. P. and Harrison, J. K. "A Set of Experiments in Thermal Similitude." NASA TMX-53346, October, 1965.

DOCUMENT CONTROL DATA - R&D

(Security classification of title, body of abstract and indexing annotation must be entered when the overall report is classified)

1 ORIGINATING ACTIVITY (Corporate author) Arnold Engineering Development Center ARO, Inc., Operating Contractor Arnold Air Force Station, Tennessee		2a REPORT SECURITY CLASSIFICATION UNCLASSIFIED	
		2b GROUP N/A	
3 REPORT TITLE SOME ASPECTS OF THERMAL MODEL TESTING IN SPACE CHAMBERS			
4 DESCRIPTIVE NOTES (Type of report and inclusive dates) N/A			
5 AUTHOR(S) (Last name, first name, initial) Nutt, K. W., and van der Bliet, J. A., ARO, Inc.			
6 REPORT DATE April 1967		7a TOTAL NO OF PAGES 27	7b NO OF REFS 6
8a CONTRACT OR GRANT NO AF40(600)-1200 b. PROJECT NO		9a. ORIGINATOR'S REPORT NUMBER(S) AEDC-TR-67-38	
c. Program Element 65402234 d.		9b OTHER REPORT NO(S) (Any other numbers that may be assigned this report) N/A	
10. AVAILABILITY/LIMITATION NOTICES Distribution of this document is unlimited.			
11 SUPPLEMENTARY NOTES Available in DDC.		12. SPONSORING MILITARY ACTIVITY Arnold Engineering Development Center, Air Force Systems Command, Arnold Air Force Station, Tennessee	
13 ABSTRACT Various facets of thermal testing of space vehicles in cold vacuum chambers, with and without solar simulation, are discussed. Emphasis is on thermal modeling of spacecraft. Thermal modeling is discussed for the case of simultaneous preservation of temperature, material and surface properties. The following specific items are treated: (1) a criterion for the application of isothermal modeling is developed and illustrated with experimental data, (2) rules for nonisothermal modeling are discussed and illustrated with experimental results, (3) the effect of internal convection is calculated and modeling rules are developed, (4) the effect of internal radiation is discussed and the relative importance illustrated theoretically, and (5) a criterion is developed for the degree of intensity nonuniformity for a solar simulator in terms of desired temperature accuracy.			

KEY WORDS

LINK A		LINK B		LINK C	
ROLE	WT	ROLE	WT	ROLE	WT

space vehicles
 environmental tests
 thermal tests
 model scaling
 isothermal modeling
 nonisothermal
 internal radiation
 solar simulation

15-7

2. Thermal modeling
 3. Space vehicles - Thermal testing
 4. Space chamber - Thermal testing

INSTRUCTIONS

1. **ORIGINATING ACTIVITY:** Enter the name and address of the contractor, subcontractor, grantee, Department of Defense activity or other organization (*corporate author*) issuing the report.

2a. **REPORT SECURITY CLASSIFICATION:** Enter the overall security classification of the report. Indicate whether "Restricted Data" is included. Marking is to be in accordance with appropriate security regulations.

2b. **GROUP:** Automatic downgrading is specified in DoD Directive 5200.10 and Armed Forces Industrial Manual. Enter the group number. Also, when applicable, show that optional markings have been used for Group 3 and Group 4 as authorized.

3. **REPORT TITLE:** Enter the complete report title in all capital letters. Titles in all cases should be unclassified. If a meaningful title cannot be selected without classification, show title classification in all capitals in parenthesis immediately following the title.

4. **DESCRIPTIVE NOTES:** If appropriate, enter the type of report, e.g., interim, progress, summary, annual, or final. Give the inclusive dates when a specific reporting period is covered.

5. **AUTHOR(S):** Enter the name(s) of author(s) as shown on or in the report. Enter last name, first name, middle initial. If military, show rank and branch of service. The name of the principal author is an absolute minimum requirement.

6. **REPORT DATE:** Enter the date of the report as day, month, year; or month, year. If more than one date appears on the report, use date of publication.

7a. **TOTAL NUMBER OF PAGES:** The total page count should follow normal pagination procedures, i.e., enter the number of pages containing information.

7b. **NUMBER OF REFERENCES:** Enter the total number of references cited in the report.

8a. **CONTRACT OR GRANT NUMBER:** If appropriate, enter the applicable number of the contract or grant under which the report was written.

8b, 8c, & 8d. **PROJECT NUMBER:** Enter the appropriate military department identification, such as project number, subproject number, system numbers, task number, etc.

9a. **ORIGINATOR'S REPORT NUMBER(S):** Enter the official report number by which the document will be identified and controlled by the originating activity. This number must be unique to this report.

9b. **OTHER REPORT NUMBER(S):** If the report has been assigned any other report numbers (*either by the originator or by the sponsor*), also enter this number(s).

10. **AVAILABILITY/LIMITATION NOTICES:** Enter any limitations on further dissemination of the report, other than those

imposed by security classification, using standard statements such as:

- (1) "Qualified requesters may obtain copies of this report from DDC."
- (2) "Foreign announcement and dissemination of this report by DDC is not authorized."
- (3) "U. S. Government agencies may obtain copies of this report directly from DDC. Other qualified DDC users shall request through _____."
- (4) "U. S. military agencies may obtain copies of this report directly from DDC. Other qualified users shall request through _____."
- (5) "All distribution of this report is controlled. Qualified DDC users shall request through _____."

If the report has been furnished to the Office of Technical Services, Department of Commerce, for sale to the public, indicate this fact and enter the price, if known.

11. **SUPPLEMENTARY NOTES:** Use for additional explanatory notes.

12. **SPONSORING MILITARY ACTIVITY:** Enter the name of the departmental project office or laboratory sponsoring (*paying for*) the research and development. Include address.

13. **ABSTRACT:** Enter an abstract giving a brief and factual summary of the document indicative of the report, even though it may also appear elsewhere in the body of the technical report. If additional space is required, a continuation sheet shall be attached.

It is highly desirable that the abstract of classified reports be unclassified. Each paragraph of the abstract shall end with an indication of the military security classification of the information in the paragraph, represented as (TS), (S), (C), or (U).

There is no limitation on the length of the abstract. However, the suggested length is from 150 to 225 words.

14. **KEY WORDS:** Key words are technically meaningful terms or short phrases that characterize a report and may be used as index entries for cataloging the report. Key words must be selected so that no security classification is required. Identifiers, such as equipment model designation, trade name, military project code name, geographic location, may be used as key words but will be followed by an indication of technical context. The assignment of links, rules, and weights is optional.